
Research Article

Endometrial CAFs Resist Effect of Antitumor Drugs in A Patient-Derived 2-Cell Hybrid Co-Culture Model

Raed Sulaiman¹, Jennifer C. Aske², Xiaoqian Lin², Adam Dale², Kris Gaster³, Luis Rojas Espallat⁴, David Starks⁴, Pradip De^{2,5,6} and Nandini Dey^{2,5,*}

Abstract

Drug resistance in tumor cells is a significant roadblock in the clinical management of advanced or recurrent diseases in endometrial cancers. As a part of the tumor-stromal ecosystem, tumor cells are ecologically connected to the cancer-associated fibroblasts (CAFs), which form contributory elements of the tumor microenvironment (TME). We recently reported a novel model of patient-derived CAF-based 2-cell Hybrid Co-Culture (HyCC) to evaluate CAFs' role in developing drug resistance and understanding personalized tumor cell-CAF dialogue. Using our 2-cell HyCC model of patient-derived endometrial CAFs, we present data to demonstrate the direct counter-inhibitory effect of CAFs to combinations of cytotoxic and targeted drugs in developing drug resistance. CAFs derived from resected endometrial tumor samples were first passage-wise characterized before and after freeze-thaw for their positive and negative CAF markers expression pattern. Paclitaxel and its combination with copanlisib, TAK228, lenvatinib, and trametinib were used to test the 3D clonogenic growth of endometrial AN3CA cells on endometrial CAFs. We demonstrate that CAF-mediated resistance to antitumor drugs occurs via direct and indirect contact with CAFs in HyCC. Our data established the strength of the 2-cell HyCC model of patient-derived CAFs in solid tumors and provided a model of resistance to antitumor drugs tailored on a patient-to-patient basis.

Keywords: Exvivo resistance Platform; CAF-mediated resistance; Combinations of cytotoxic and targeted drugs.

Simple Summary: The major impediment to the clinical management of advanced or recurrent diseases in endometrial cancers is the development of drug resistance. The development of resistance is a complex process involving the temporal and special events with the tumor and the host's stromal compartments. Since no patient's tumor is similar to the other patient, and so are the stromal compartments. This poses a limitation in the study of the mechanisms of the development of drug resistance using a generalized model system. To overcome this hurdle, we have recently developed a model to test the mechanism of drug resistance in a patient-specific manner using one of the significant elements of the stromal compartments of individual patients. This element is called cancer-associated fibroblast. Our novel model allows us to test the drug effects in a Hybrid Co-Culture system comprised of an individual patient-derived cancer-associated fibroblast in the presence of endometrial tumor cells. In this study, we present the result of treatment with drug combinations using this model. We demonstrate that the resistance to antitumor drugs occurs via direct and indirect contact with cancer-associated

Affiliation:

¹Department of Pathology, Avera McKennan Hospital, Sioux Falls, SD, USA

²Translational Oncology Laboratory, Avera Research Institute, Sioux Falls, SD, USA

³Assistant VP Outpatient Cancer Clinics, Avera Cancer Institute, Sioux Falls, SD, USA

⁴Department of Gynecologic Oncology, Avera Research Institute, Sioux Falls, SD, USA

⁵Department of Internal Medicine, University of South Dakota SSOM, Sioux Falls, SD, USA

⁶Viecure, Greenwood Village, Colorado, USA

*Corresponding author:

Nandini Dey, Senior Scientist, Director of Translational Oncology Laboratory, Avera Research Institute, 1000 E 23rd Street, Sioux Falls, SD, 57105, USA.

Citation: Raed Sulaiman, Jennifer C. Aske, Xiaoqian Lin, Adam Dale, Kris Gaster, Luis Rojas Espallat, David Starks, Pradip De, and Nandini Dey. Endometrial CAFs Resist Effect of Antitumor Drugs in A Patient-Derived 2-Cell Hybrid Co-Culture Model. *Journal of Cancer Science and Clinical Therapeutics*. 8 (2024): 147-166.

Received: May 30, 2024

Accepted: June 05, 2024

Published: July 20, 2024

fibroblasts. Our model will provide a test tool to understand the dialogue between tumor cell and cancer-associated fibroblast in a patient-specific manner toward managing advanced disease in endometrial cancers.

Introduction

The development of drug resistance and the failure to mitigate the resistance are directly associated with progression and adverse outcomes in gynecological cancers. There are limitations associated with the chemotherapeutic drugs used to garner the management of advanced and recurrent endometrial cancers. The resistance to drugs in the adjuvant setting is challenging as more than 25% of patients with a stage > 1 invasive disease subsequently progress as a metastatic disease in endometrial cancers [1]. Refractory and resistant tumor cells present within the residual disease have thus been linked with primary adverse outcomes. The Cancer Genome Atlas (TCGA) presents a classification of endometrial cancers into four molecular subtypes whose treatment consideration is now recommended. In advanced staged endometrial cancers, relapse occurs despite surgery, hormone therapy, and chemotherapy [2]. Tumor cells within the tumor mass are known to be part of the tumor-TME (tumor microenvironment) ecosystem. Although the mutational make-up of tumor cells is the primary determinant of treatment outcome and predicts patient survival, recent studies prove that tumor evolution in space, time, and treatment depends on the close interaction of mutagenized tumor cells with their TME [3]. Cancer-associated fibroblasts are critical features of TME [4]. The essential role of cancer-associated fibroblasts (CAFs) within the tumor stroma has been associated with developing resistance to drugs in various solid tumors, including endometrial cancers, and is an emerging field in cancer biology [5, 6]. CAF tumor cell crosstalk and CAF's crosstalk with the rest of TME components, angiogenic and immunogenic, is a *bête noire* of therapy and determines disease prognosis [7]. Thus, understanding the mechanism of CAF-mediated drug resistance holds power to address the challenge of resistance via disrupting the CAF-tumor dialogue. The key to knowing how to disrupt the CAF-tumor dialogue is gaining knowledge about the conversation in a patient-specific manner. We have recently designed a patient-derived CAF-based 2-cell Hybrid Co-Culture (HyCC) model to test the effect of CAF on endometrial tumor cells [8]. Using HyCC, we present the data to demonstrate the direct counter-inhibitory effect of CAFs on combinations of cytotoxic and targeted drugs. To the best of our knowledge, no study has been conducted to test the effect of patient-derived primary endometrial CAFs on the clonogenic growth of endometrial tumor cells. Our data demonstrate that the HyCC model of CAF can be employed to test the drug-resisting property of CAFs on a patient-to-patient basis, indicating the translational significance and utility of the model in functional precision medicine.

Materials & Methods

Patient consent & tissue collection

The institutional and/or licensing committee approved all experimental protocols. Informed consent(s) (IRB approved: Protocol Number Study: 2017.053- 100399_ExVivo001) was obtained from patients. Resected unfixed tumor tissue(s) were received from the pathology department. The tissues were collected during surgery in designated collection media as per the guidelines and relevant regulations and provided by the pathologist, depending upon the availability of the tissue on a case-to-case basis. The primary cultures of CAFs were set up from the resected samples of tumors from patients with endometrial cancers, as per the guidelines and relevant regulations provided by the pathologist who performed the grossing. Samples were collected in DMEM/F-12 + Glutamax 500mL (base) supplemented with HyClone Penicillin-Streptomycin 100X 100mL (1%). We have included all consecutive patients who provided informed consents. Only pathologically determined tumors of an identified cancerous histology were included. As suggested by the reviewer, we have included the following supplementary table (S1) to indicate the stages and different histological parameters of the 44 patients included in the study as identified by our pathologist (Supplementary Table 1).

Cell lines and reagents

Fibroblast cells (Human uterine fibroblasts HUF; Primary Uterine Fibroblasts, Cat # PCS-460-010) and endometrial tumor cells (RL-95-2 and AN3CA) were bought from AATC and were culture according to the ATCC recommended method. Antibodies for ICC were from Cell Marque, NOVUS, Abcam, Agilent- Dako, and Cell Signaling. All cells within mid-passages (7-8) used for the study were tested negative for mycoplasma. The antibodies for WB were bought from Cell Signaling, USA. We chose Fibroblast cells (Human uterine fibroblasts HUF; Primary Uterine Fibroblasts, Cat # PCS-460-010) to compare different markers of patient-derived CAFs in primary cultures with the human uterine fibroblasts both for the standardization and characterization purposes. We included two endometrial tumor cells (RL-95-2 and AN3CA) to co-culture with patient-derived CAFs. They also served as negative controls both for the standardization and characterization purposes.

1.1.1 Drug of choice: We used paclitaxel (20nM), combination A (20nM paclitaxel+100nM Copanlisib), combination B (20nM paclitaxel+ 200nM TAK228), combination C (20nM paclitaxel+ 200nM Lenvatinib), combination D (20nM paclitaxel+ 200nM Trametinib), and combination E (200nM Copanlisib) for the study (Supplementary Table S3). Copanlisib Clinical benefit of copanlisib monotherapy has been reported in uterine cancers. Recently an NRG Oncology Phase II study (NRG-

GY008) evaluated copanlisib, an α and δ isoform-specific phosphoinositide 3-kinase (PI3K) inhibitor, in patients with persistent or recurrent endometrial carcinoma harboring PIK3CA hotspot mutations (a very common somatic mutations in endometrial cancer along with PTEN mutation). Patients with deleterious PTEN mutations without PTEN protein loss may benefit from treatment with the pan-PI3K inhibitor copanlisib. The study was conducted as a part of the NCI-MATCH trial as sub-protocol Z1H. NCI-MATCH is a large national precision oncology trial with more than 1,100 sites involved. The study contains arms with specific targeted therapies for patients whose tumors have matching underlying molecular alterations that are deemed to be associated with sensitivity to these specific treatments (Targeted Oncology November 2, 2021). Our study was initiated before the FDA (Food and Drug Administration) approval of alpelisib (p110 alpha selective inhibitor) and PTEN mutation is one of the key resistance mechanisms of alpelisib. Hence we hypothesized that copanlisib is the choice of drug for PI3K pathway alterations (either PIK3CA or PTEN somatic mutation), which are frequently altered in endometrial cancers. Sapanisertib (CB-228/TAK-228) is a potent, selective ATP competitive, next-generation dual inhibitor of mTORC1/2. The PI3K/v-AKT Murine Thymoma Viral Oncogene (AKT)/mTOR pathway plays a diverse role in regulation of several cellular functions such as cellular growth, proliferation, and survival. This pathway is frequently dysregulated in various cancers, such as endometrial, cervical, lung, prostate, skin, and breast cancers, and mTOR is a key node and central regulator in this pathway. mTOR exists in two physically and functionally distinct protein signaling complexes, one with raptor, which is sensitive to the mTOR inhibitor rapamycin, and the other with rictor, which is rapamycin insensitive. The rapalogs, such as everolimus, exert their inhibitory action predominantly via mTORC1, while their inhibitory effect on mTORC2 is limited or weak. Consequently, continued signaling through significant pathway feedback loops, results in upregulation of AKT, which has them undesirable effect of accelerating cell proliferation, antagonizing the anti-proliferative effect of mTOR inhibition. Thus, next-generation dual inhibitors of mTORC1 and mTORC2 have been developed, and preclinical models have supported the potency of this dual inhibition strategy. Lenvatinib is a targeted treatment, not a chemotherapy drug. A targeted cancer treatment works by affecting specific target molecules that lead to the growth and spread of cancer. Lenvatinib is a multiple kinase inhibitor against the VEGFR1, VEGFR2 and VEGFR3 kinases, which blocks cell proteins and signals directed at blood vessels that help the cancer to survive. Evidence and efficacy of tyrosine kinase inhibitor in combinations with pembrolizumab plus lenvatinib have been reported in several advanced solid cancers, including endometrial cancers. Indeed pembrolizumab plus lenvatinib was recently approved for the treatment of advanced or recurrent endometrial carcinoma

in women with disease progression on or following prior treatment with a platinum - containing therapy in any setting, including 1st-line of treatment. Trametinib, a MEK1/2 inhibitor, as a class, may represent an attractive treatment option for variety of solid tumors, given that patients without the BRAFV600E mutation typically have downstream mutations in the MAPK pathway including KRAS. The MEK inhibitor trametinib is of particular interest, given its selectivity and potency, and we hypothesize based on the published literature in gynecological cancers that it could provide another effective option for targeted therapy (<https://doi.org/10.1182/bloodadvances.2022009013>). In endometrial cancers, the most commonly practiced clinical strategies for the management of the disease involve surgery, followed by a combination of chemotherapy (paclitaxel, carboplatin/cisplatin, and doxorubicin/liposomal doxorubicin) radiation therapy alone or combined with hormonal therapy (American Cancer Society guidelines). Paclitaxel is routinely used along with platinum agents to treat advanced endometrial cancers, and the administration of paclitaxel (weekly) as a single agent to patients with recurrent or metastatic disease is the most commonly practiced approach in clinics (<https://www.cancer.org/> accessed on 12 December 2022). According to the NCCN (National Comprehensive Cancer Network®) guidelines, one of the FDA- approved targeted therapies include multi-TKI, lenvatinib, and anti-angiogenic bevacizumab, with the recent inclusion of immunotherapy, pembrolizumab with lenvatinib, or dostarlimab for high TMB, MSI- high dMMR tumors. In the current study, we chose paclitaxel alone and in combination (As Combo Match) with several pathway-targeted agents including copanlisib, TAK228, lenvatinib, and trametinib.

Establishment of patient-specific ex vivo tumor-endometrial caf-2-cell model of hybrid co-culture (HyCC)

We established and characterized the primary culture of CAF from the resected tumor tissues from patients (TCAF here off used interchangeably with CAF) [9]. As mentioned, we established a novel matrigel-based On-Top 2-cell HyCC model [8]. The DiO and DiI, were used for the 3D matrigel On-Top clonogenic assays. HyCC consisted of preparatory and experiment phases, as mentioned earlier. In short, the experiment phase included (1) 24 hours plating of DiO-CAFs, (2) plating of DiI-stained tumor cells on DiO-CAFs with and without paclitaxel and five combos (Combo A, Combo B, Combo C, Combo D, Combo E) as mentioned in the Table 1 in 3D formats. A parallel single-cell culture was set up separately to test the effect of the individual drug combo(s) on CAF and AN3CA cells. The HyCC was set up in quadruplicates. The media was changed every 2 days. The double-fluorescence signals from the live cells in cultures were recorded along with bright field photomicrographs

at different time points using dry-objectives of Olympus BX43 Microscope using cellSens 1.18 LIFE SCIENCE IMAGING SOFTWARE (OLYMPUS CORPORATION). Photomicrographs were taken on day 0+ (within 4 hours for the 3D format as pictures are difficult to focus at zero hours in 3D) and on day 7. Semi-quantification was performed based on the fluorescence intensities of DiI tumor cells on DiO-TCAFs/NCAFs from 5–6 random microscopic fields of independent experiments (performed in quadruplicates). Statistical significance was determined by calculating Student's t-test at $p < 0.05$.

Effect of cafs on paclitaxel alone and in combination with targeted antitumor drugs using 2-cell hybrid co-culture model

We then evaluated the effect of CAF on the tumoricidal effect of paclitaxel and its combination with targeted drugs (Table 1) by plating AN3CA in HyCC on TCAF in 3D format. To test the autocrine and paracrine effect of CAF in resisting the effect of paclitaxel and targeted drugs in HyCC, we evaluated the effect of drugs on both (1) direct contact with the CAF and (2) non-direct contact with CAF. Direct contact with the CAF and tumor cells was tested by plating AN3CA cells on the CAF-coated coverslips. In contrast, a non-direct contact with CAF comprised of AN3CA cells was placed on the plate outside the circumference of CAF-coated coverslips in the same HyCC wells as schematically presented in Figure 1A.

The model was used to test the effect of the antitumor and/or anti-angiogenic drugs (A). We present the results of a direct-contact effect versus a non-direct-contact effect of CAF using Hybrid Co-culture using the effect of paclitaxel (B). A direct-contact effect was tested by taking the photomicrographs focused on the DiO-CAF coated cover- clips within the HyCC (Left two panels of Figure 1B). A non-direct-contact effect was tested by taking the photomicrographs focused on the plate area outside the DiO- CAF coated cover-clips within the HyCC (Right two panels of figure 1B). The “non- direct-contact” model was achieved by placing and co-culturing the cells in the presence or absence of drugs, wherein the two types of cell populations are physically barred from a

Table 1: List of the drug combinations tested to demonstrate the protective effect of endometrial CAFs on the 3D Matrigel growth of endometrial cancer cells in HyCC.

Combination* #	Drugs used for the Combination
A	Paclitaxel plus Copanlisib
B	Paclitaxel plus TAK228
C	Paclitaxel plus Lenvatinib
D	Paclitaxel plus Trametinib
E	Copanlisib

*The combinations are referred in the text as Combo A, Combo B, Combo C, Combo D, and Combo E.

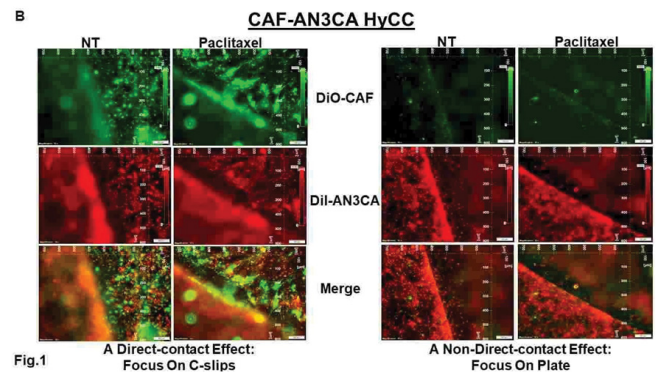
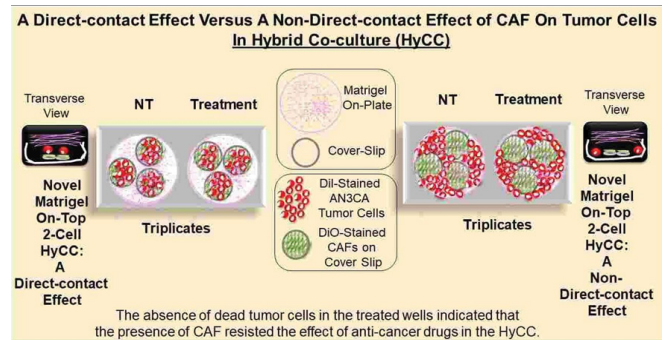


Figure 1: Schematic plan to demonstrate a direct-contact effect versus a non- direct-contact effect of CAF using Hybrid Co-culture (HyCC):

direct cell-to-cell contact; one cell population was plated on the cover slips and the other was plated on the plates during co-culture. Since the co- culture was carried out in the same media, the effect/no-effect of the testing drug under such experimental condition happened not by a direct cell (CAFs) to cell (endometrial cells) contact but via the paracrine action of the secreted substances from one cell (CAFs) in the media to the other types of cells (endometrial cells) during the period of co-culture. The purpose of focusing on the coverslip in the left panel of the figure is to demonstrate the effect of the drug on tumor cells when they are in direct contact with CAFs (coated on the coverslips) in HyCC. The purpose of focusing on the plate in the right panel in the figure is to demonstrate the effect of the drug on tumor cells when they are NOT in direct contact with CAFs (since CAFs are coated ONLY on the coverslips and tumor cells are not in direct contact with CAFs) in HyCC.

Results

Patient information

Our cohort involved a total of 53 patients with endometrial cancers who participated in the study and provided informed consent. The information about the patients included in the study has been presented earlier [9]. In short, CAFs were established from samples received at the time of surgery. Out of 53 tissue samples, a total of 44 tissue samples were used for establishing CAF cultures.

Ex vivo primary culture of cafs and marker-based verification of CAF

Characterization and validation of the primary culture of TCAF in the ex vivo culture were performed based on expression (ICC, qRT-PCR, WB, and flow cytometry) of positive and negative markers, as mentioned earlier [9]. In short, TCAFs were positive markers of CAF, including SMA, FAP, TE-7, and S100A4, while they were always negative for EpCAM and CK 8,18 (a positive marker of epithelial tumor cells), CD31 (endothelial marker) and CD45 (LCA marker for leucocytes).

Patient-specific ex vivo model of hybrid co-culture (HyCC)

We first evaluated the growth pattern of endometrial tumor cells on TCAFs in two 3D formats of HyCC, (1) a direct contact format and (2) a non-contact format, as diagrammatically presented in Figure 1. Figure 1 represents a schematic plan to demonstrate our experimental design to test a direct-contact effect versus a non-direct-contact effect of CAF using Hybrid Co-culture (HyCC): The model was used to test the effect of the antitumor and/or anti-angiogenic drugs (A). A direct contact effect is tested by first plating the CAFs on cover slips. Once the cover-slips were placed inside the 6-well plates, the endometrial tumor cells were plated on them. Thus a direct cell-to-cell contact between the two types of cell pupolation was established. On the contrary, when the CAF coated coverslips were placed on endometrial cell plated 6-wells no direct cell-to-cell contact between the CAFs and endometrial tumor cell pupolation was established. Thus any effect observed was understood as a paracrine (relating to, promoted by, or being a substance secreted by a cell and acting on adjacent cells which are not essentially in direct physical contact) effect. We present the results of a direct-contact effect versus a non-direct-contact effect of CAF using Hybrid Co-culture using the effect of paclitaxel (B). A direct-contact effect was tested by taking the photomicrographs focused on the DiO - CAF coated cover-clips within the HyCC (Left two panels of Figure 1B). A non-direct-contact effect was test-ed by taking the photomicrographs focused on the plate area outside the DiO-CAF coated cover-clips within the HyCC (Right two panels of figure 1B). The HyCC was designed to test the effect of patient-derived ex vivo CAFs, one of the critical components of TME, on the growth and proliferation of endometrial tumor cells. The design of the experiment included (1) a direct-contact effect and (2) a non-direct-contact effect of CAFs on the 2D and 3D growth of tumor cells in the presence and absence of anti-tumor drug, paclitaxel alone or in combination using HyCC (Fig.1). The primary CAFs derived from resected endometrial tumor tissues as well as endometrial tumor cells were labeled live with different high-performance fluorescent lipophilic tracers (Vybrant DiI and DiO). The effect of the presence and absence

of CAFs was evaluated on the growth of tumor cells in 3D On-Top clonogenic HyCC in the presence of anti-tumor drugs. Cover slips were coated with DiO-CAF. A direct contact effect was tested by taking the photomicrographs of fluorescently labeled cells in HyCC focused on the DiO-CAF-coated cover slips within the HyCC. A non-direct-contact effect was tested by taking the photomicrographs focused on the plate area outside the DiO-CAF-coated cover slips. We observed that growth of (1) AN3CA cells was higher on day 7 as compared to day 0+ in both the formats of HyCC (Figure 2A & B) and (2) both AN3CA and CAFs are enhanced on day 7 of the single cell culture (Figure 2C). Photomicrographs of Figure 2 show the clonogenic growth of AN3CA is significantly higher on day 7 compared to Day 0+. When we grew the AN3CA cells for 7 days, the cells grew in colonies typically showing a clonogenic growth which can be clearly observed from the merged photomicrographs on the right most panels. Since the cells could not be photographed immediately after plating we provided time for the cells to get attached to the substratum before taking the pictures, hence we used the term, Zero+ hour. The treatment with paclitaxel decreased the growth of AN3CA cells in a single-cell AN3CA-only culture. Since we have previously reported the effect of paclitaxel on 3D Matrigel growth of AN3CA cells plated on CAF [9], the validity of the HyCC formats here was confirmed by testing the effect CAF on the effect of paclitaxel (Figure 3) as an internal validation control of drug effect as compared to the non-treated vehicle control (Figure 2) at day 7.

Effect of CAFs in Resisting Paclitaxel in Combination with Pathway- Targeted Drugs

We used two separate culture platforms, HyCC and a parallel single-cell culture platform. The design included (1) two types of cell types, DiO-CAF and DiI- AN3CA cells, (2) five treatment combos (Combo A, Combo B, Combo C, Combo D, and Combo E; Table 1), (3) two culture modes of HyCC, HyCC On-Coverslips, and HyCC On-Plates and (4) two-time points, Zero+ hour and 7 days. The growth inhibitory effect of paclitaxel was used as the baseline in measuring the role of CAF in resisting paclitaxel's growth inhibitory effect in combination with pathway- targeted drugs Combo A, Combo B, Combo C, Combo D, and Combo E on endometrial tumor cells. Figure 4 shows that although treatment with paclitaxel in combination with copanlisib (Combo A) blocked the growth of AN3CA cells on day 7 in the single cell culture, the presence of CAF significantly blocked the growth inhibitory effect of the combination. The growth of CAF in the single cell culture is not altered. Figure 4A provided both zero day and 7-day controls for the comparison. It shows that (1) CAFs grow after 7 days as compared to Zero+ hour (left panel), and AN3CA grows mostly in colonies (with cells piling on top of each other due to the apparent loss of contact inhibition common for epithelial tumor cells) after 7 days as

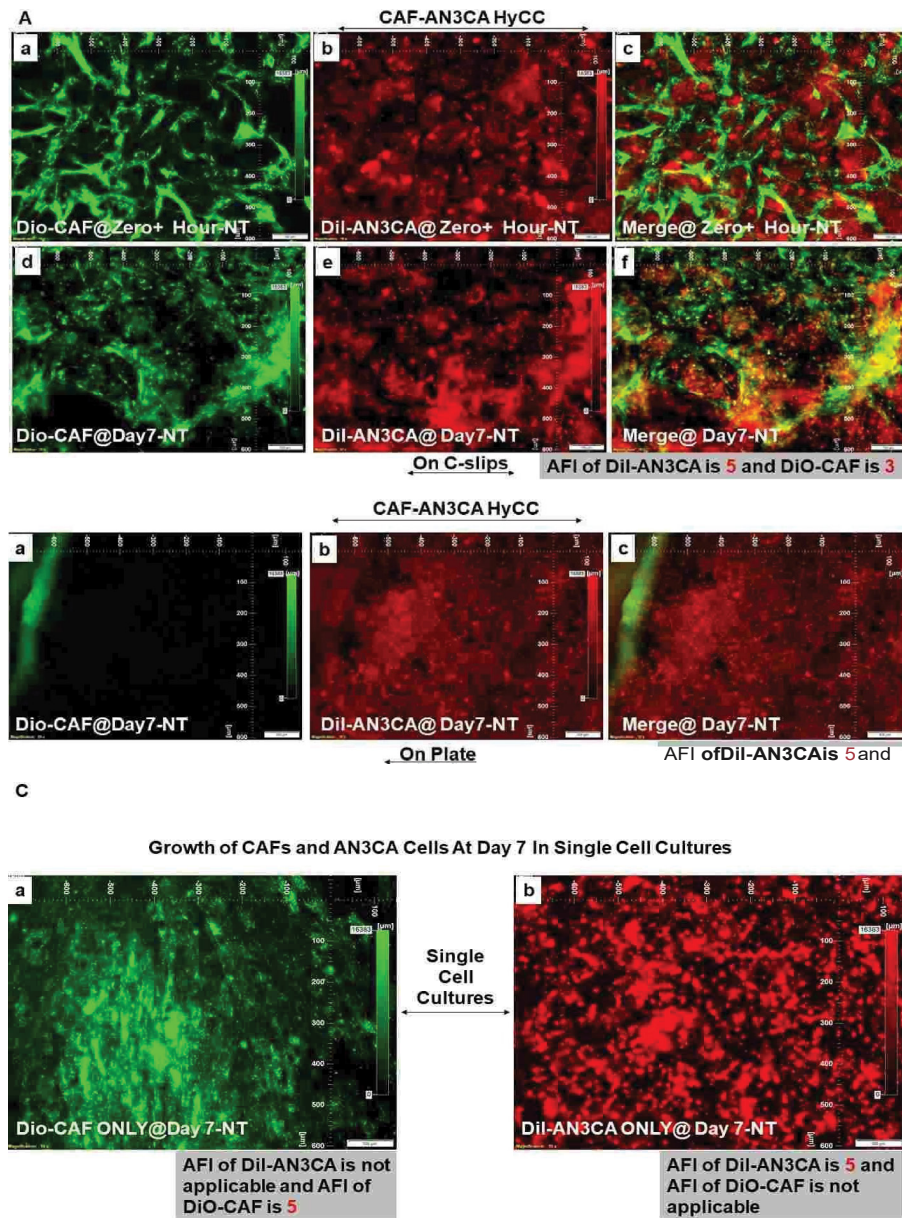


Figure 2: Growth of AN3CA cells on patient-derived CAF for 7 days in 3D Matrigel HyCC: CAF derived from the primary culture of resected tumor tissue samples from patients with endometrial cancers were stained with DiO- fluorescence stain. DiI-stained AN3CA cells were plated 24 hours after on DiO- CAF-coated coverslips. Photomicrographs were taken on zero+ hours (upper panel of A) of the plating of AN3CA cells on DiO-CAF coated coverslips and (lower panel of A) as well as on the cells on-plate (panel of B) on day 7. The growth of AN3CA cells in 3D on-matrigel alone on day 7 is presented (C right photomicrograph) compared to the growth of DiO-CAF (C left photomicrograph). Paclitaxel was more affective in the endometrial cells. However when the same cells were co-cultured in the presence of patient-derived CAFs, the effect of paclitaxel was attenuated as compared to the effect of paclitaxel on the endometrial cells alone. Figure 2 demonstrates the growth of AN3CA cells on patient-derived CAF for 7 days in 3D Matrigel HyCC. CAF from tumors from patients with endometrial cancers were stained with DiO-fluorescence stain. DiI- stained AN3CA cells were plated 24 hours after on DiO-CAF-coated coverslips. Photomicrographs were taken on zero+ hours (upper panel of A) of the plating of AN3CA cells on DiO-CAF coated coverslips and (lower panel of A) as well as on the cells on-plate (panel of B) on day 7. The growth of AN3CA cells in 3D on- matrigel alone on day 7 is presented (C right photomicrograph) compared to the growth of DiO-CAF (C left photomicrograph). Semi-quantification (as expressed by Arbitrary Fluorescent Intensity: AFI) was performed based on the % fluorescence intensities of DiI-AN3CA cells and DiO-CAF from 5–6 random microscopic fields of independent experiments (performed in quadruplicates) at different times. Statistical significance was determined by calculating the Student’s t-test at $p < 0.05$. Conditional formatting was performed using a 3-color scale (Table 2), red being the highest/maximum, violet being the no change, and green being the lowest/minimum values in the arbitrary scale. Positive numbers in combination with the red color indicated a high (5), medium (3), and low (1) percentage of increase. In contrast, negative numbers in combination with the green color indicated a high (-5), medium (-3), and low (-1) percentage of decrease. The Violet color indicated no change. The individual slides of the figure of fluorescent images are labeled separately (a-f as appropriate).

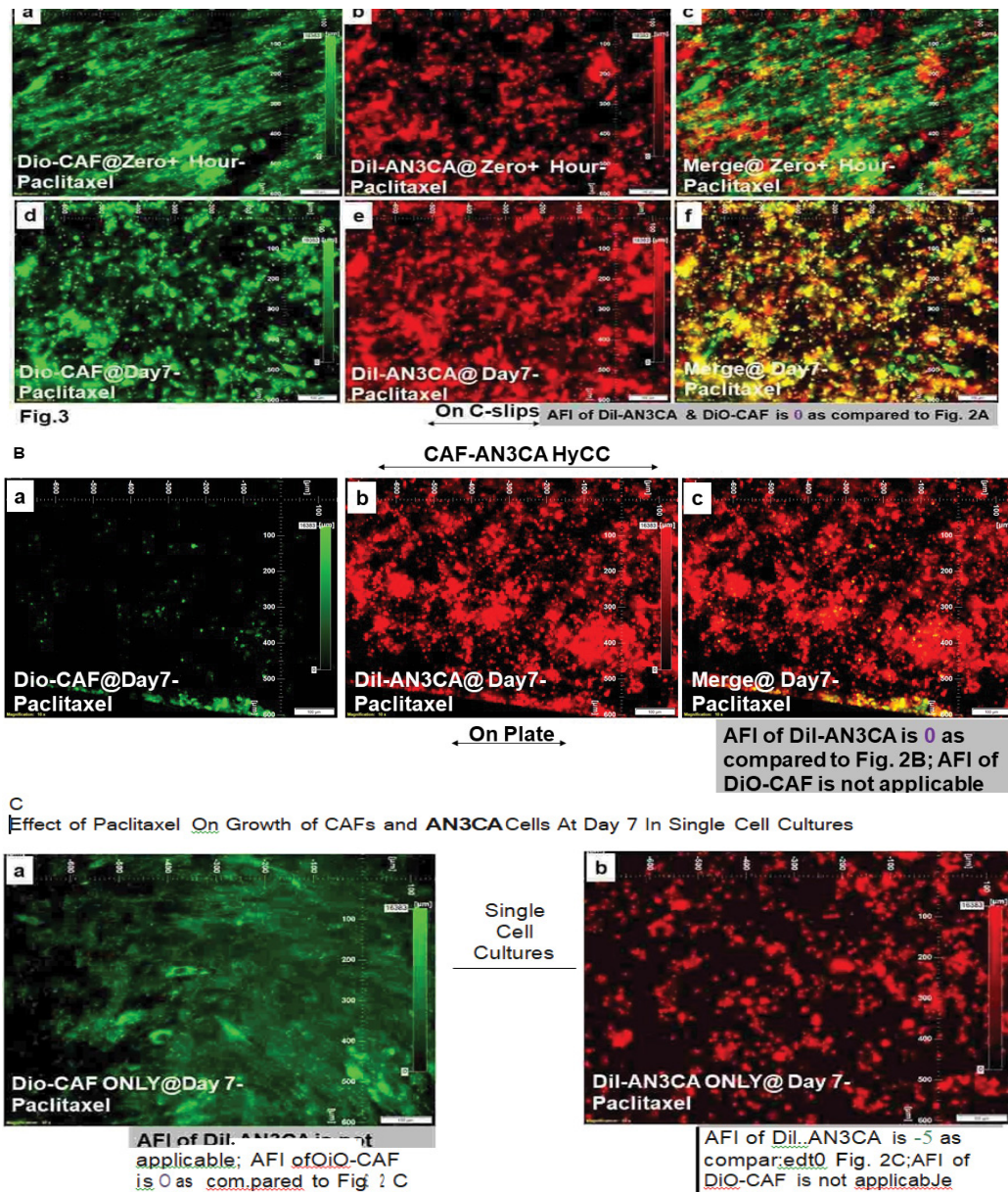


Figure 3: Effects of patient-derived primary CAF on the antitumor effect of paclitaxel in Hybrid Co-Culture: Protective effect of CAF (DiO-stained; green fluorescent color) against the tumoricidal effect of paclitaxel on AN3CA cells (DiI- stained; orange-red fluorescent color) is demonstrated from the photomicrographs of live cells plated on CAF-coated coverslips (direct contact with CAF) (A) as well as on-plate (non-direct contact with CAF) (B) in 3D matrigel HyCC. The growth inhibitory effect of paclitaxel in 3D on-matrigel growth of DiI-AN3CA alone on day 7 is presented in the picture (C right photomicrograph) as compared to the no-effect on the growth of DiO-CAF (C left photomicrograph). Figure 3 presents the effects of patient-derived primary CAF on the antitumor effect of paclitaxel in Hybrid Co-Culture. Protective effect of CAF (DiO-stained; green fluorescent color) against the tumoricidal effect of paclitaxel on AN3CA cells (DiI-stained; orange-red fluorescent color) is demonstrated from the photomicrographs of live cells plated on CAF-coated coverslips (direct contact with CAF) (A) as well as on-plate (non-direct contact with CAF) (B) in 3D matrigel HyCC. The growth inhibitory effect of paclitaxel in 3D on-matrigel growth of DiI-AN3CA alone on day 7 is presented in the picture (C right photomicrograph) as compared to the no-effect on the growth of DiO-CAF (C left photomicrograph). Semi-quantification (as expressed by Arbitrary Fluorescent Intensity: AFI) was performed based on the % fluorescence intensities of DiI-AN3CA cells and DiO-CAF from 5–6 random microscopic fields of independent experiments (performed in quadruplicates) at different times. Statistical significance was determined by calculating the Student's t-test at $p < 0.05$. Conditional formatting was performed using a 3-color scale (Table 2), red being the highest/maximum, violet being the no change, and green being the lowest/ minimum values in the arbitrary scale. Positive numbers in combination with the red color indicated a high (5), medium (3), and low (1) percentage of increase. In contrast, negative numbers in combination with the green color indicated a high (-5), medium (-3), and low (-1) percentage of decrease. The Violet color indicated no change. The individual slides of the figure of fluorescent images are labeled separately (a-f as appropriate).

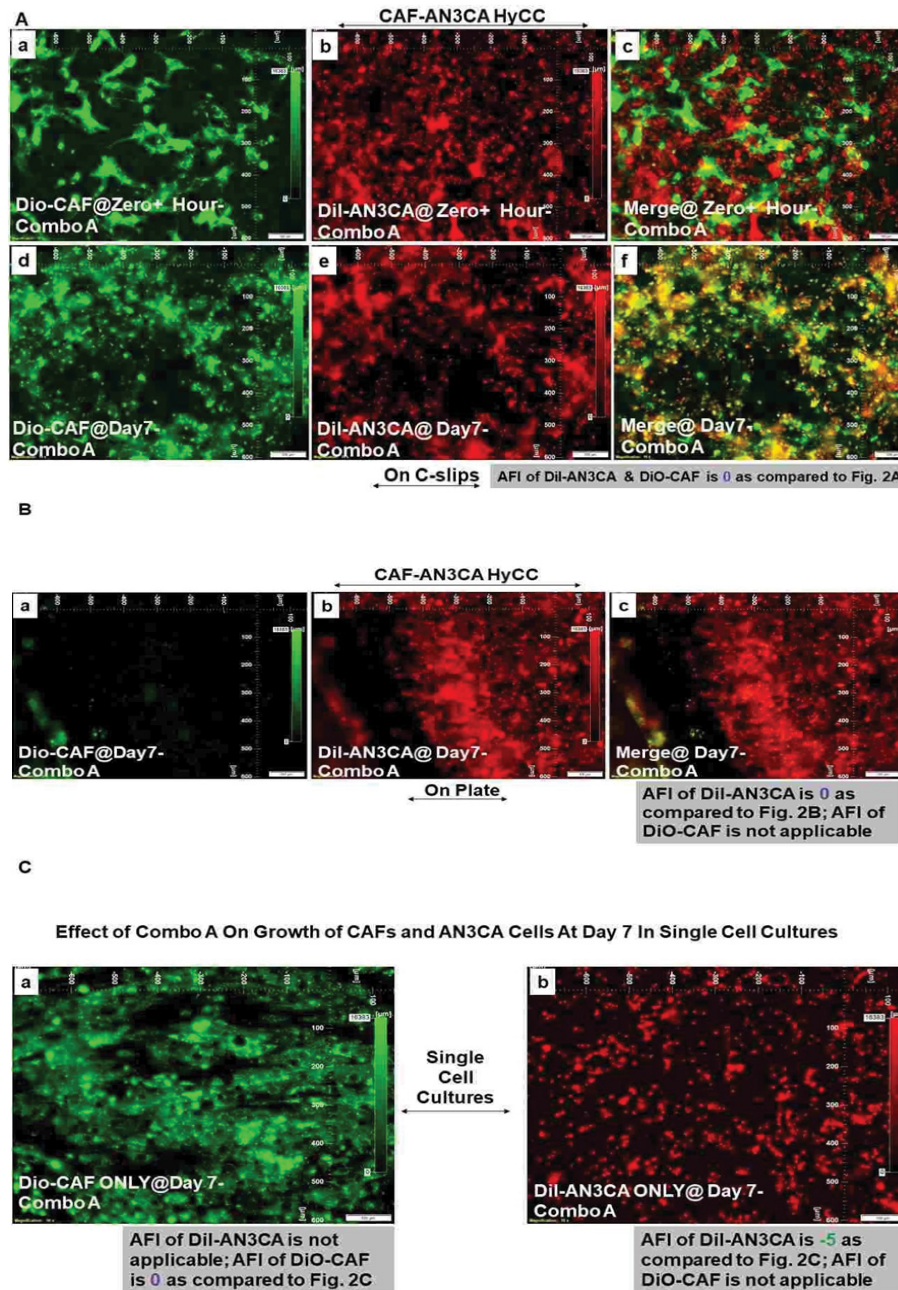


Figure 4: Effects of patient-derived primary CAF on the antitumor effect of paclitaxel in combination with Copanlisib (Combo A) in Hybrid Co-Culture: Protective effect of CAF (DiO-stained; green fluorescent color) against the tumoricidal effect of paclitaxel in combination with Copanlisib (Combo A) on AN3CA cells (DiI-stained; orange-red fluorescent color) is demonstrated from the photomicrographs of live cells plated on CAF-coated coverslips (direct contact with CAF) (A) as well as on-plate (non-direct contact with CAF) (B) in 3D matrigel HyCC. The growth inhibitory effect of paclitaxel in combination with Copanlisib (Combo A) in 3D on-matrigel growth of DiI-AN3CA alone on day 7 is presented in the picture (C right photomicrograph) as compared to the no-effect on the growth of DiO-CAF (C left photomicrograph). CAF resisted the growth inhibitory effect of paclitaxel in combination with Copanlisib (Combo A) on AN3CA in a HyCC 3D format. Semi-quantification (as expressed by Arbitrary Fluorescent Intensity: AFI) was performed based on the % fluorescence intensities of DiI-AN3CA cells and DiO-CAF from 5–6 random microscopic fields of independent experiments [performed in quadruplicates) at different times [(Arbitrary Scale Based On % Change In The Relative Fluorescence Intensity (DiI-AN3CA & DiO-CAF)]. Statistical significance was determined by calculating the Student's t-test at $p < 0.05$. Conditional formatting was performed using a 3-color scale, red being the highest/maximum, violet being the no change, and green being the lowest/minimum values in the arbitrary scale. Positive numbers in combination with the red color indicated a high (5), medium (3), and low (1) percentage of increase (wherever applicable). In contrast, negative numbers in combination with the green color indicated a high (-5), medium (-3), and low (-1) percentage of decrease (wherever applicable). The Violet color indicated no change. The individual slides of the figure of fluorescent images are labeled separately (a-f as appropriate).

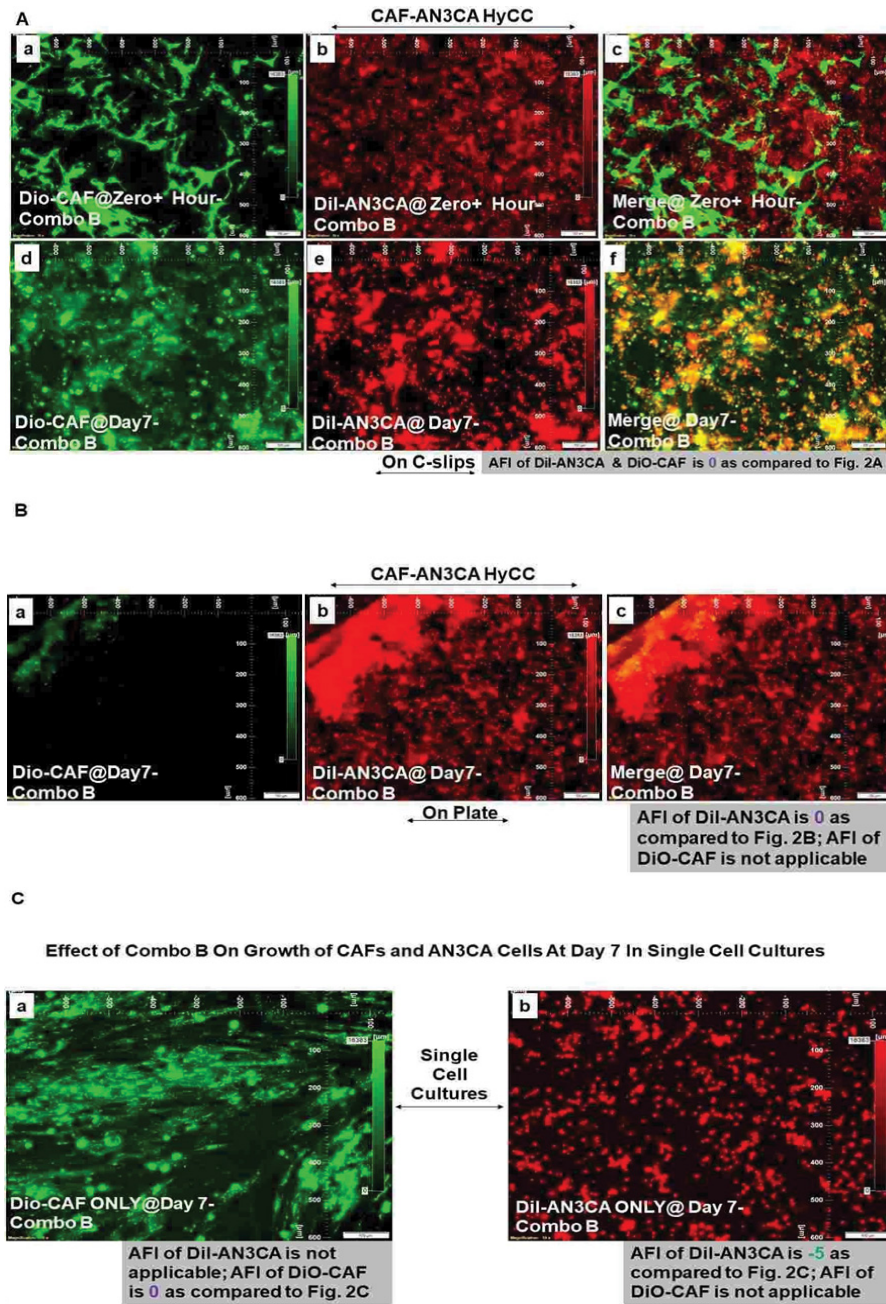


Figure 5: Effects of patient-derived primary CAF on the antitumor effect of paclitaxel in combination with TAK228 (Combo B) in Hybrid Co-Culture: Protective effect of CAF (DiO-stained; green fluorescent color) against the tumoricidal effect of paclitaxel in combination with TAK228 (Combo B) on AN3CA cells (DiI-stained; orange-red fluorescent color) is demonstrated from the photomicrographs of live cells plated on CAF-coated coverslips (direct contact with CAF) (A) as well as on-plate (non-direct contact with CAF) (B) in 3D matrigel HyCC. The growth inhibitory effect of paclitaxel in combination with TAK228 (Combo B) in 3D on-matrigel growth of DiI-AN3CA on day 7 is presented in the picture (C right photomicrograph) as compared to the no-effect on the growth of DiO-CAF (C left photomicrograph). CAF resisted the growth inhibitory effect of paclitaxel in combination with TAK228 (Combo B) on AN3CA in a HyCC 3D format. Semi-quantification (as expressed by Arbitrary Fluorescent Intensity: AFI) was performed based on the % fluorescence intensities of DiI-AN3CA cells and DiO-CAF from 5–6 random microscopic fields of independent experiments [performed in quadruplicates] at different times [(Arbitrary Scale Based On % Change In The Relative Fluorescence Intensity (DiI-AN3CA & DiO-CAF)]. Statistical significance was determined by calculating the Student's t-test at $p < 0.05$. Conditional formatting was performed using a 3-color scale, red being the highest/maximum, violet being the no change, and green being the lowest/minimum values in the arbitrary scale. Positive numbers in combination with the red color indicated a high (5), medium (3), and low (1) percentage of increase (wherever applicable). In contrast, negative numbers in combination with the green color indicated a high (-5), medium (-3), and low (-1) percentage of decrease (wherever applicable). The Violet color indicated no change. The individual slides of the figure of fluorescent images are labeled separately (a-f as appropriate).

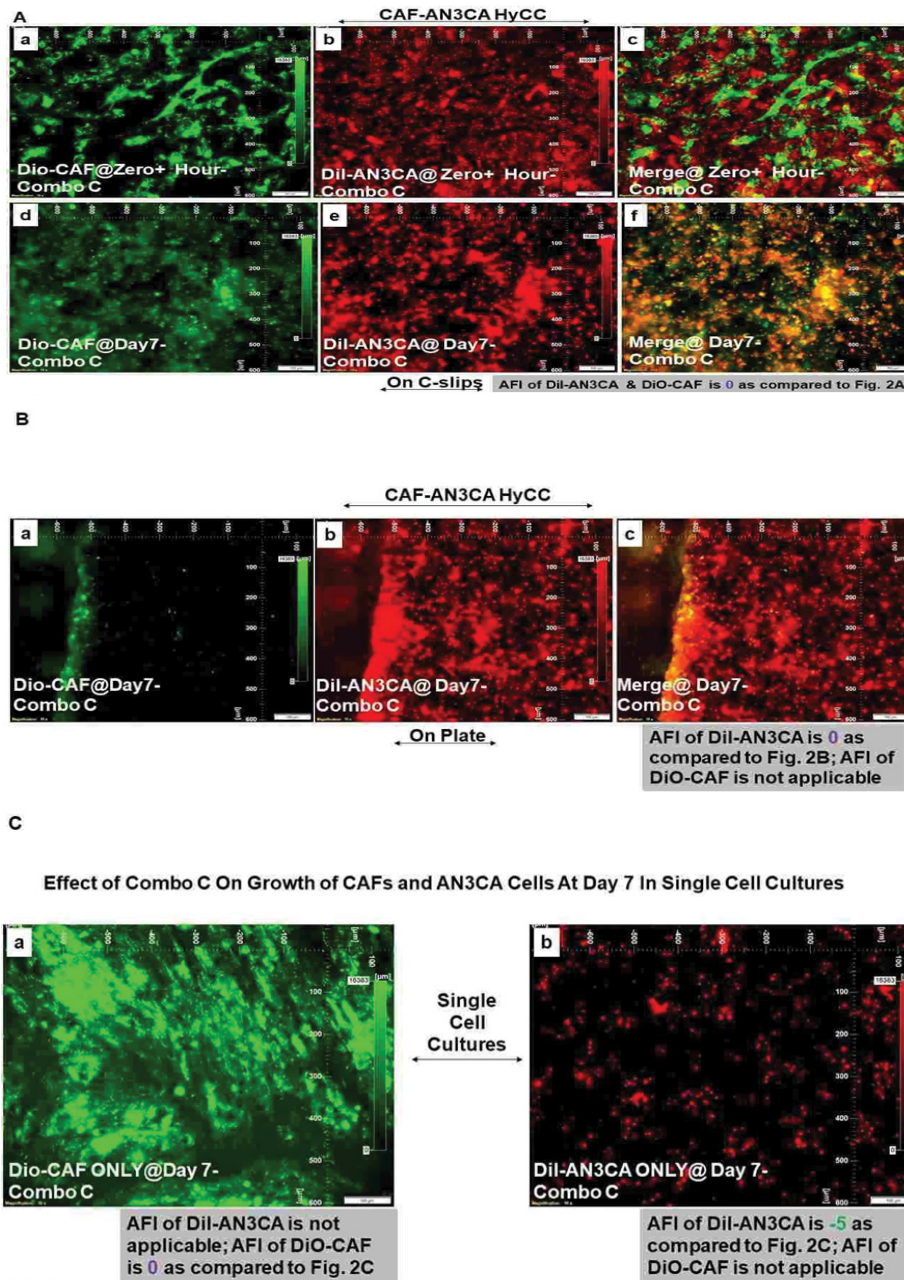


Figure 6: Effects of patient-derived primary CAF on the antitumor effect of paclitaxel in combination with Lenvatinib (Combo C) using Hybrid Co-Culture: Protective effect of CAF (DiO-stained; green fluorescent color) against the tumoricidal effect of paclitaxel in combination with Lenvatinib (Combo C) on AN3CA cells (DiI-stained; orange-red fluorescent color) is demonstrated from the photomicrographs of live cells plated on CAF-coated coverslips (direct contact with CAF) (A) as well as on-plate (non-direct contact with CAF) (B) in 3D matrigel HyCC. The growth inhibitory effect of paclitaxel in combination with Lenvatinib (Combo C) in 3D on-matrigel growth of DiI-AN3CA alone on day 7 is presented in the picture (C right photomicrograph) as compared to the no-effect on the growth of DiO-CAF (C left photomicrograph). CAF resisted the growth inhibitory effect of paclitaxel in combination with Lenvatinib (Combo C) on AN3CA in a HyCC 3D format. Semi-quantification (as expressed by Arbitrary Fluorescent Intensity: AFI) was performed based on the % fluorescence intensities of DiI-AN3CA cells and DiO-CAF from 5–6 random microscopic fields of independent experiments [performed in quadruplicates) at different times [(Arbitrary Scale Based On % Change In The Relative Fluorescence Intensity (DiI-AN3CA & DiO-CAF)]. Statistical significance was determined by calculating the Student's t-test at $p < 0.05$. Conditional formatting was performed using a 3-color scale, red being the highest/maximum, violet being the no change, and green being the lowest/minimum values in the arbitrary scale. Positive numbers in combination with the red color indicated a high (5), medium (3), and low (1) percentage of increase (wherever applicable). In contrast, negative numbers in combination with the green color indicated a high (-5), medium (-3), and low (-1) percentage of decrease (wherever applicable). The Violet color indicated no change. The individual slides of the figure of fluorescent images are labeled separately (a -f as appropriate).

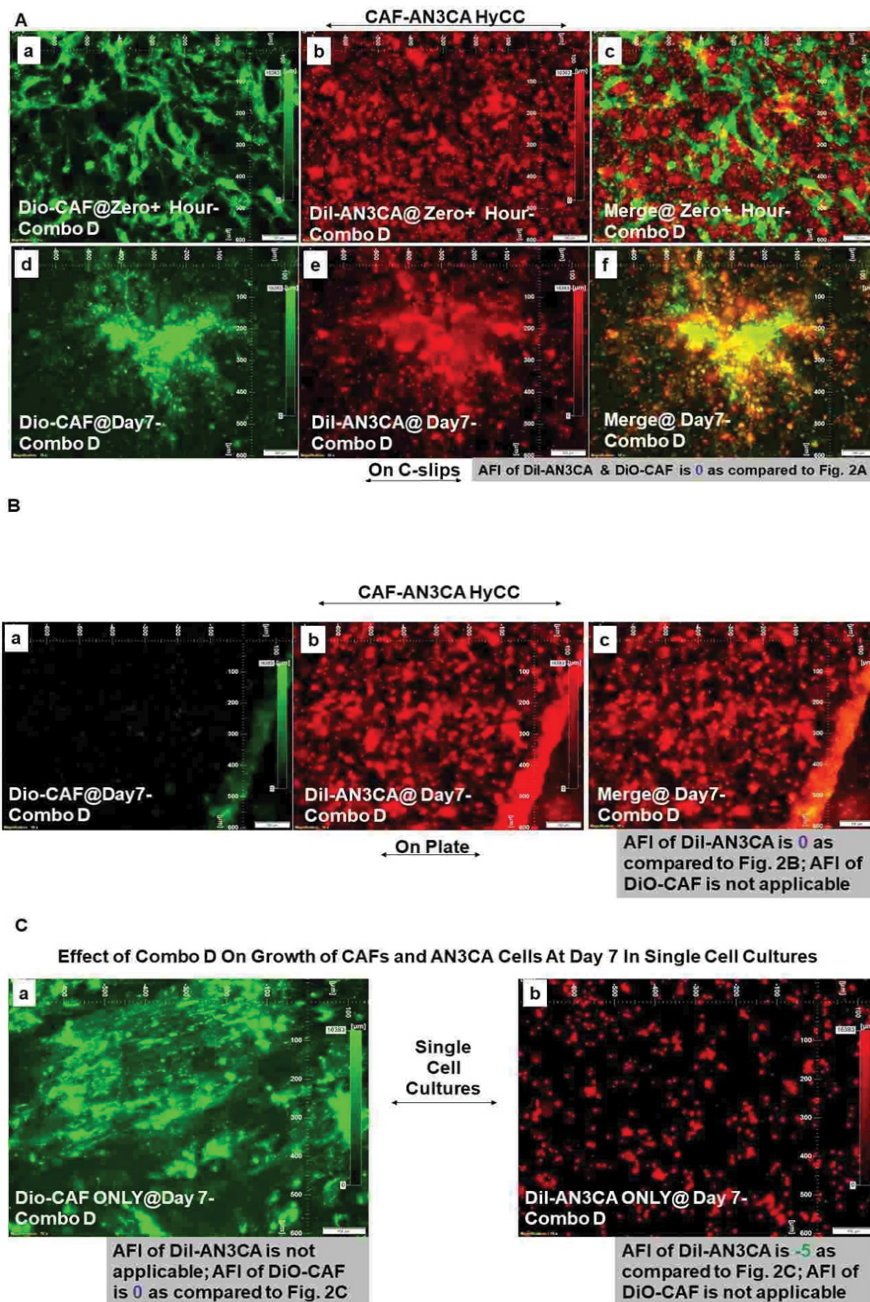


Figure 7: Effects of patient-derived primary CAF on the antitumor effect of paclitaxel in combination with Trametinib (Combo D) in Hybrid Co-Culture: Protective effect of CAF (DiO-stained; green fluorescent color) against the tumoricidal effect of paclitaxel in combination with Trametinib (Combo D) on AN3CA cells (DiI-stained; orange-red fluorescent color) is demonstrated from the photomicrographs of live cells plated on CAF-coated coverslips (direct contact with CAF) (A) as well as on-plate (non-direct contact with CAF) (B) in 3D matrigel HyCC. The growth inhibitory effect of paclitaxel in combination with Trametinib (Combo D) in 3D on-matrigel growth of DiI-AN3CA alone on day 7 is presented in the picture (C right photomicrograph) as compared to the no-effect on the growth of DiO-CAF (C left photomicrograph). CAF resisted the growth inhibitory effect of paclitaxel in combination with Trametinib (Combo D) on AN3CA in a HyCC 3D format. Semi-quantification (as expressed by Arbitrary Fluorescent Intensity: AFI) was performed based on the % fluorescence intensities of DiI-AN3CA cells and DiO-CAF from 5–6 random microscopic fields of independent experiments [performed in quadruplicates) at different times [(Arbitrary Scale Based On % Change In The Relative Fluorescence Intensity (DiI-AN3CA & DiO-CAF)]. Statistical significance was determined by calculating the Student's t-test at $p < 0.05$. Conditional formatting was performed using a 3-color scale, red being the highest/maximum, violet being the no change, and green being the lowest/minimum values in the arbitrary scale. Positive numbers in combination with the red color indicated a high (5), medium (3), and low (1) percentage of increase (wherever applicable). In contrast, negative numbers in combination with the green color indicated a high (-5), medium (-3), and low (-1) percentage of decrease (wherever applicable). The Violet color indicated no change. The individual slides of the figure of fluorescent images are labeled separately (a-f as appropriate).

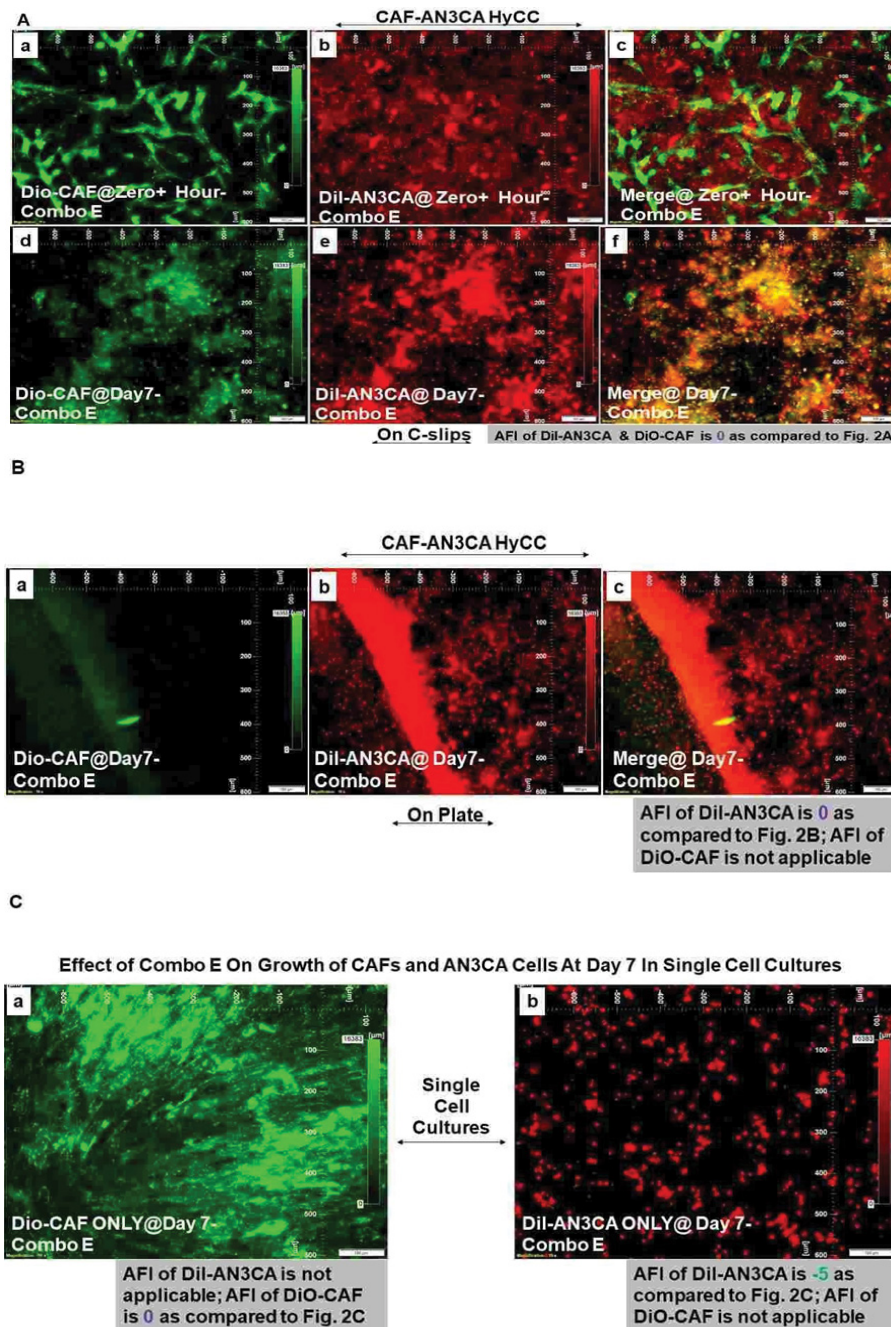


Figure 8: Effects of patient-derived primary CAF on the antitumor effect of copanlisib (Combo E) in Hybrid Co-Culture: Protective effect of CAF (DiO-stained; green fluorescent color) against the tumoricidal effect of copanlisib (Combo E) on AN3CA cells (DiI-stained; orange-red fluorescent color) is demonstrated from the photomicrographs of live cells plated on CAF-coated coverslips (direct contact with CAF) (A) as well as on-plate (non-direct contact with CAF) (B) in 3D matrigel HyCC. The growth inhibitory effect of copanlisib (Combo E) in 3D on-matrigel growth of DiI-AN3CA on day 7 is presented in the picture (C right photomicrograph) as compared to the no-effect on the growth of DiO-CAF (C left photomicrograph). CAF resisted the growth inhibitory effect of copanlisib (Combo E) on AN3CA in a HyCC 3D format. Semi-quantification (as expressed by Δ Arbitrary Fluorescent Intensity: AFI) was performed based on the % fluorescence intensities of DiI-AN3CA cells and DiO-CAF from 5–6 random microscopic fields of independent experiments [performed in quadruplicates) at different times [(Arbitrary Scale Based On % Change In The Relative Fluorescence Intensity (DiI- AN3CA & DiO-CAF)]. Statistical significance was determined by calculating the Student’s t-test at $p < 0.05$. Conditional formatting was performed using a 3-color scale, red being the highest/maximum, violet being the no change, and green being the lowest/minimum values in the arbitrary scale. Positive numbers in combination with the red color indicated a high (5), medium (3), and low (1) percentage of increase (wherever applicable). In contrast, negative numbers in combination with the green color indicated a high (-5), medium (-3), and low (-1) percentage of decrease (wherever applicable). The Violet color indicated no change. The individual slides of the figure of fluorescent images are labeled separately (a-f as appropriate).

Table 2: Conditional Formatting of Grades based on the Arbitrary Scale of the relative % of Fluorescence Intensity of DiI-AN3CA Cells and DiO-CAF. DiO- CAFs are plated on coverslips.

Cell Type(s) Involved in the Experiment	Treatment Type (s)	Culture Platform Type(s)	End-Time of the Experiment	Comparison Type(s)	Photo-micrographs Presented in Figure #	Grades* (Arbitrary Scale Based on the % of Fluorescence Intensity of DiI-AN3CA)	Grades* (Arbitrary Scale Based on the % of Fluorescence Intensity of DiO-CAF)
DiO-CAF & DiI-AN3CA	Vehicle Control (NT)	HyCC On Cover slips (DiO-CAF)	Day 7	Day Zero+ vs Day7	Fig. 2A	5	3
DiI-AN3CA		HyCC On Plates		Day7 as compared to Day Zero+	Fig. 2B	5	Not Applicable (Focused On-Plate)
DiI-AN3CA		Single Cell Cultures		Day7 as compared to Day Zero+	Fig. 2C (Right Panel)	5	Not Applicable
DiO-CAF				Day7 as compared to Day Zero+	Fig. 2C (Left Panel)	Not Applicable	5
Cell Type(s) Involved in the Experiment	Treatment Type (s)	Culture Platform Type(s)	End-Time of the Experiment	Comparison Type(s)	Photo-micrographs Presented in Figure #	Grades* (Arbitrary Scale Based on the % of Fluorescence Intensity of DiI-AN3CA)	Grades* (Arbitrary Scale Based on the % of Fluorescence Intensity of DiO-CAF)
DiO-CAF & DiI-AN3CA	Pacli-taxel	HyCC On Cover slips (On DiO-CAF)	Day 7	Drug Treatment Vs. No Treatment	Fig. 3A vs. Fig. 2A	0	0
DiI-AN3CA		HyCC On Plates			Fig. 3B vs. Fig. 2B	0	Not Applicable (Focused On-Plate)
DiI-AN3CA		Single Cell Cultures			Fig. 3C (Right Panel) vs. Fig.2C (Right Panel)	-5	Not Applicable
DiO-CAF					Fig. 3C (Left Panel) vs Fig.2C (Left Panel)	Not Applicable	0
Cell Type(s) Involved in the Experiment	Treatment Type (s)	Culture Platform Type(s)	End-Time of the Experiment	Comparison Type(s)	Photo-micrographs Presented in Figure #	Grades* (Arbitrary Scale Based on the % of Fluorescence Intensity of DiI-AN3CA)	Grades* (Arbitrary Scale Based on the % of Fluorescence Intensity of DiO-CAF)

DiO-CAF& Dil-AN3CA	Pacli-taxel + Copan-lisib (Combo A)	HyCC On Cover slips (On DiO-CAF)	Day 7	Drug Treatment Vs. No Treatment	Fig. 4A vs. Fig. 2A	0	0
Dil-AN3CA		HyCC On Plates			Fig. 4B vs. Fig. 2B	0	Not Applicable (Focused On-Plate)
Dil-AN3CA		Single Cell Cultures			Fig. 4C (Right Panel) vs. Fig.2C (Right Panel)	-5	Not Applicable
DiO-CAF					Fig. 4C (Left Panel) vs Fig.2C (Left Panel)	Not Applicable	0
Cell Type(s) Involved in the Experiment	Treatment Type (s)	Culture Platform Type(s)	End-Time of the Experiment	Comparison Type(s)	Photo-micrographs Presented in Figure #	Grades* (Arbitrary Scale Based on the % of Fluorescence Intensity of Dil-AN3CA)	Grades* (Arbitrary Scale Based on the % of Fluorescence Intensity of DiO-CAF)
DiO-CAF & Dil-AN3CA	Pacli-taxel + TAK 228 (Combo B)	HyCC On Cover slips (On DiO-CAF)	Day 7	Drug Treatment Vs. No Treatment	Fig. 5A vs. Fig. 2A	0	0
Dil-AN3CA		HyCC On Plates			Fig. 5B vs. Fig. 2B	0	Not Applicable (Focused On-Plate)
Dil-AN3CA		Single Cell Cultures			Fig. 5C (Right Panel) vs. Fig.2C (Right Panel)	-5	Not Applicable
DiO-CAF					Fig. 5C (Left Panel) vs Fig.2C (Left Panel)	Not Applicable	0
Cell Type(s) Involved in the Experiment	Treatment Type (s)	Culture Platform Type(s)	End-Time of the Experiment	Comparison Type(s)	Photo-micrographs Presented in Figure #	Grades* (Arbitrary Scale Based on the % of Fluorescence Intensity of Dil-AN3CA)	Grades* (Arbitrary Scale Based on the % of Fluorescence Intensity of DiO-CAF)

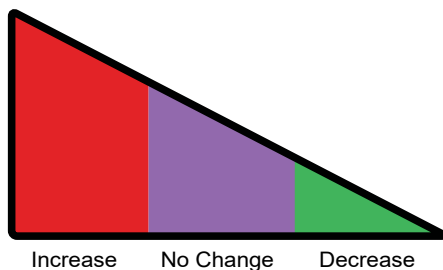
DiO-CAF & Dil-AN3CA	Pacli-taxel + Lenva-tinib (Combo C)	HyCC On Cover slips (On DiO-CAF)	Day 7	Drug Treatment Vs. No Treatment	Fig. 6A vs. Fig. 2A	0	0
Dil-AN3CA		HyCC On Plates			Fig. 6B vs. Fig. 2B	0	Not Applicable (Focused On-Plate)
Dil-AN3CA		Single Cell Cultures			Fig. 6C (Right Panel) vs. Fig.2C (Right Panel)	-5	Not Applicable
DiO-CAF					Fig. 6C (Left Panel) vs Fig.2C (Left Panel)	Not Applicable	0
Cell Type(s) Involved in the Experi-ment	Treat- ment Type (s)	Culture Platform Type(s)	End- Time of the Exper- iment	Comparison Type(s)	Photo- micrographs Presented in Figure #	Grades* (Arbitrary Scale Based on the % of Fluorescence Intensity of Dil- AN3CA)	Grades* (Arbitrary Scale Based on the % of Fluorescence Intensity of DiO- CAF)
DiO-CAF & Dil-AN3CA	Pacli-taxel + Trame-tinib (Combo D)	HyCC On Cover slips (On DiO-CAF)	Day 7	Drug Treatment Vs. No Treatment	Fig. 7A vs. Fig. 2A	0	0
Dil-AN3CA		HyCC On Plates			Fig. 7B vs. Fig. 2B	0	Not Applicable (Focused On-Plate)
Dil-AN3CA		Single Cell Cultures			Fig.7C (Right Panel) vs. Fig.2C (Right Panel)	-5	Not Applicable
DiO-CAF					Fig. 7C (Left Panel) vs Fig.2C (Left Panel)	Not Applicable	0
Cell Type(s) Involved in the Experi-ment	Treat- ment Type (s)	Culture Platform Type(s)	End- Time of the Exper- iment	Comparison Type(s)	Photo- micrographs Presented in Figure #	Grades* (Arbitrary Scale Based on the % of Fluorescence Intensity of Dil- AN3CA)	Grades* (Arbitrary Scale Based on the % of Fluorescence Intensity of DiO- CAF)

DiO-CAF & DiI-AN3CA	Copan-lisib (Combo E)	HyCC On Cover slips (On DiO-CAF)	Day 7	Drug Treatment Vs. No Treatment	Fig. 8A vs. Fig. 2A	0	0
DiI-AN3CA		HyCC On Plates	Day 7		Fig. 8B vs. Fig. 2B	0	Not Applicable (Focused On-Plate)
DiI-AN3CA		Single Cell Cultures	Day 7		Fig. 8C (Right Panel) vs. Fig. 2C (Right Panel)	-5	Not Applicable
DiO-CAF			Day 7		Fig. 8C (Left Panel) vs. Fig. 2C (Left Panel)	Not Applicable	0

*Semi-quantification was performed based on the % fluorescence intensities of DiI-AN3CA cells and DiO-CAF from 5–6 random microscopic fields of independent experiments (performed in quadruplicates) at different times. Statistical significance was determined by calculating the Student's t-test at $p < 0.05$. Conditional formatting was performed using a 3-color scale, red being the highest/maximum, violet being the no change, and green being the lowest/minimum values in the arbitrary scale. Positive numbers in combination with the red color indicated a high (5), medium (3), and low (1) percentage of increase. In contrast, negative numbers in combination with the green color indicated a high (-5), medium (-3), and low (-1) percentage of decrease.

Scale for Table 2: Arbitrary Scale Based On % Change In The Relative Fluorescence Intensity (DiI-AN3CA & DiO-CAF).

High	Medium	Low	No change	Low	Medium	High
Increase				Decrease		
75-100%	25-74%	1-24%	0%	24-1%	74-25%	100-75%
5	3	1	0	-1	-3	-5



compared to Zero+ hour (mid panel) in an “cover-slip” culture (where both CAFs and AN3CA are in direct contact with each other). The right panel shows the merge (please note that the typical clonogenic growth of AN3CA cells on and around CAFs appear yellow in the merged photomicrographs). The Figure 4B is a photomicrograph of “on-plate” culture. The CAFs are plated on the cover slips

only. While the AN3CA cells were cultured on the plate. That is why the CAFs are not visible when the object of the microscope was focused on the plate. Please note that CAFs were visible in figure 4A which is a representation of an “on cover slips” culture. The experiments were repeated in 4-6 times and photomicrographs were taken of the randomly chosen fields from each independent experimental setup. Likewise, treatment with paclitaxel in combination with TAK228 (Combo B), lenvatinib (Combo C), and trametinib (Combo D) as well as copanlisib only (Combo E), although blocked the growth of AN3CA in single cell culture, had failed to inhibit the growth of AN3CA in HyCC with CAF in both on-coverslip and on-plate formats (Figure 5-8). The summarized results with the conditional formatted semi-quantified data are presented in Table 2. The result indicated that the effect of CAF is mediated not via direct contact with the AN3CA cells but via the paracrine secretory mechanism. Table 2 semi-quantitatively demonstrated that a HyCC with CAF had a similar protecting effect on paclitaxel and pathway-targeted drugs on clonogenic growth of AN3CA, while none of the drugs had significant growth inhibitor effects on CAF in a single cell culture. In summary, our data show that endometrial CAF confers a protective effect on endometrial tumor cells against the chemotherapy drug paclitaxel in combination with different pathway-targeted drugs in HyCC.

Discussion

The Cancer Genome Atlas (TCGA) presents a classification of endometrial cancers into four molecular subtypes whose treatment consideration is now recommended [10]. The molecular characterization of endometrial cancer has paved the way for the development of novel combinations of immunotherapies and pathway-targeted therapies, leading to the approval of immune checkpoint inhibitors (combination of lenvatinib plus pembrolizumab) [11]. Our cohort consisted predominantly of patients with endometrioid adenocarcinoma, with fewer patients with high-grade serous carcinomas of both papillary and mixed types (see Table 1 of [9]). Paclitaxel is routinely used (weekly) as a single agent to patients with recurrent or metastatic disease is the most commonly practiced approach in the clinics [12] (<https://www.cancer.org/>). Carboplatin plus paclitaxel is the established frontline treatment for advanced/recurrent disease [11]. We have chosen the combinations of paclitaxel with pathway-targeted drugs based on the primary pathway alterations in these cancers and the list of effective combinations from our ex vivo testing of drug effects in endometrial cancers (Table 3). Considering the recent knowledge about the role of TME-CAF in mediating drug resistance in solid tumors, we hypothesized that the drug (adjuvant) mediated resistance in endometrial cancers is contributed by the CAF component of TME. We tested the effect of drug combinations on endometrial tumor samples in ex vivo cultures. Out of several combinations tested, we observed anti-proliferative and pro-apoptotic effects in certain combinations (submitted for publication). Hence, in this study, we tested the function of CAF from the tumor samples, which was affected by our studies ex vivo drug treatment. Our data provides experimental proof of "Deadlock game" as explained in non-small cell lung cancer [13]. Our results demonstrate that drug treatment decreased the 3D growth of endometrial tumor cells in matrigel in a single-cell culture, while the presence of CAF in HyCC resisted the growth inhibitor effect of the drugs, alone or in combinations (Table 2). We present the data of a direct-contact effect versus a non-direct-contact effect of CAF using HyCC using (Figure 1B). A direct-contact effect was tested by taking the photomicrographs focused on the DiO-CAF coated coverslips within the HyCC. A non-direct-contact effect was tested by taking the photomicrographs focused on the plate area outside the DiO-CAF-coated coverslips within the HyCC. Figure 1A shows how the experiment was designed, and Fig. 1B shows how the design was experimentally achieved. Our study demonstrated that while paclitaxel alone or in combination with targeted drugs had the anti-tumor effect in regular culture, the treatment with the same drugs failed to produce an effect in the presence of patient-derived CAFs in HyCC. The mechanism of the cell death and the mode of CAF's action is critical to further evaluate the development of the resistance and being studied using this model.

The AN3CA cells were used both alone as well as in HyCC with CAFs. Also, this formats were tested in both a 2D (absence of matrigel) or a 3D (presence of matrigel) culture systems. We determined the dosage of paclitaxel for treatment of endometrial cells, AN3CA based on the IC50. We tested the effect of CAFs on effect of paclitaxel in AN3CA cells (plated with CAF) using both 2D (absence of matrigel) or 3D (presence of matrigel) culture systems. The rationale behind the stating the effect of paclitaxel on the AN3CA cells alone versus AN3CA cells plated on patient-derived CAFs is to provide experimental evidence that the presence of CAF (direct or indirect contact) attenuates the effectiveness of the effect of paclitaxel on endometrial cells in co-cultures (with CAFs). Our data demonstrate for the first

Table 3: List of drugs (Single/Combinations) tested in ex vivo culture on tumor samples resected from patients with endometrial cancers.

List of drugs (Single/Combinations) Tested on Resected Tumor Tissue Samples from Patients with Endometrial Cancers in Ex Vivo Cultures	
Combinations Tested On Resected tumor Samples of Endometrial Cancers	Copanlisib
	Paclitaxel
	Trametinib
	Carboplatin + Paclitaxel
	Carboplatin + Paclitaxel + Cabozantinib
	Carboplatin + Paclitaxel + Lenvatinib
	Carboplatin + Paclitaxel + Ripretinib
	Carboplatin + Paclitaxel + TAK228
	Carboplatin + Paclitaxel + Trametinib
	Carboplatin + Paclitaxel + Lenvatinib + Alpelisib
	Carboplatin + Paclitaxel + Lenvatinib + Ripretinib
	Carboplatin + Paclitaxel + TAK228 + Ripretinib
	Carboplatin + Paclitaxel + TAK228 + Lenvatinib
	Carboplatin + Paclitaxel + Trametinib + Lenvatinib
	Paclitaxel + AZD6482
	Paclitaxel + Buparlisib
	Paclitaxel + Cabozantinib
	Paclitaxel + Copanlisib
	Paclitaxel + Erdafitinib
	Paclitaxel + Everolimus
	Paclitaxel + Lenvatinib
	Paclitaxel + Panobinostat
	Paclitaxel + TAK228
	Paclitaxel + Trametinib
	Paclitaxel + Cabozantinib + Everolimus
	Paclitaxel + Cabozantinib + TAK228
	Paclitaxel + Copanlisib + Panobinostat
	Paclitaxel + Lenvatinib + Trametinib
	Paclitaxel + Panobinostat + Trametinib
	Paclitaxel + TAK228 + Erdafitinib
Paclitaxel + TAK228 + Lenvatinib	
Paclitaxel + TAK228 + Panobinostat	
Paclitaxel + TAK228 + Tazemetostat	
Paclitaxel + TAK228 + Trametinib	
Paclitaxel + Trametinib + Copanlisib	

time that the presence of CAFs imparts a resistance to the tumoricidal effect of chemotherapeutic agent, paclitaxel on the endometrial cells. As expected, all figures displaying "on plate" images in the co-culture system on day 7 are with minimal to no CAFs because these images represent the cells on plate in the green fluorescent channel (used for DiO-CAF). Since DiO-CAF were plated on the cover slips only, when the objective of the microscope was focused on the "on-plate" area of the HyCC, no green signal was observed as no DiO-CAF were present on plate.

Although the growth of CAF was not significantly altered following the treatment of drugs in HyCC or single cell culture, we observed a characteristic morphological pattern of the CAFs in HyCC. The fact that the protective effect of CAF was observed simultaneously both in a direct-contact format and an indirect-contact format of HyCC proves that the mechanism of function of CAF involves a paracrine action. In fact, several studies have reported the role of CAF-derived exosomes in cancer progression [14] by regulating the survival and proliferation of cancer cells [15]. Moreover, crosstalk between CAF and immune cells of TME [16] has been implicated as the basis of CAF's clinical and therapeutic relevance [17]. CAFs have been beginning to present a deterministic role in influencing disease outcomes [17]. CAF-inclusive treatment is just beginning to broaden drug design and target the TME [6]. A number of studies provided evidence in favor of a CAF-inclusive therapy for clinical management of the disease, tumor growth, disease progression, therapeutic resistance, immune therapy, and angiogenesis [17-20]. In line with the above fact, several CAF-directed/inclusive clinical trials have been currently instituted and are ongoing in the NIH (<https://clinicaltrials.gov/ct2/home>). Although a majority of these clinical trials are initiated in advanced/metastatic tumors (ClinicalTrials.gov Identifier: NCT05547321), including hepatocellular carcinomas and neoplasms of the breast, colon, prostate, lung, ovary, and PDAC (ClinicalTrials.gov Identifier: NCT05262855), CAF-directed clinical trials in endometrial cancers are rare. Recently, we have studied the role of CAFs in the development of resistance to anti-angiogenic drugs in ovarian cancers. We have recently published the first report demonstrating a correlation between the post-surgical event and the aggressive nature of CAFs in endometrial cancers, providing an undeniable reason to study the in-depth mechanism of CAF function toward developing treatment resistance in endometrial cancers [9]. Here, we tested the hypothesis that the addition of an essential TME component, CAF, which is known to be involved in the poor prognosis, could provide more predictive models. Indeed, the result confirmed the role of CAF on tumor cell survival in the face of antitumor drug combinations. The strength of the work lies in the fact that our model has the unique capacity to test the possibility of developing resistance

to the drug in a high-risk individual patient who has been adjuvantly treated with the same drug(s). This is achieved because the CAFs are derived from the resected tumor tissue of that individual patient. Such an argument is strengthened by our recently published article demonstrating the clinical relevance of endometrial CAFs and their correlation between Post-Surgery Events and resistance to drugs and the role of patient-derived primary CAF in mediating resistance to anti-angiogenic drugs in ovarian cancers [9]. The study's limitation is that the total number of patients enrolled in the entire study was around 200. The inclusion of further patients is required to expand the study to solid tumors beyond gynecological cancers, including breast and lung cancers. Our data collectively provides a compelling experimental proof-of-concept for the protective role of CAF towards tumor cells against anti-angiogenic and antitumor drugs in gynecological cancers. We have retrospectively conducted the clinicopathological assessment of the progression of the disease following the surgery and influences of CAF's behavior and their response to chemotherapy. We have recently published the work entitled "Characterization and Clinical Relevance of Endometrial CAFs: Correlation between Post-Surgery Event and Resistance to Drugs" [9] which demonstrated that a positive correlation was found between patients with grade 3 ($p = 0.025$) as well as stage 3/4 diseases ($p = 0.0106$) bearing aggressive CAFs and the PSE. Our study is the first to report a correlation between the PSE and the aggressive nature of CAFs in endometrial cancers and provides an undeniable reason to study the in-depth mechanism of CAF function towards the development of treatment resistance in endometrial cancers.

Conclusion

The study of the development of resistance and its management in a patient-specific manner is a challenge. Such a challenge is further aggravated by the fact that no patients' tumor and TME components are similar. Hence, they respond to drugs differently as they evolve throughout the disease progression. Our CAF-based 2-cell Hybrid Co-Culture (HyCC) was designed to evaluate CAFs' role in developing drug resistance and understanding personalized tumor cell - CAF dialogue. In our study, paclitaxel and its combination with copanlisib, TAK228, lenvatinib, and trametinib were used to test the 3D clonogenic growth of endometrial AN3CA cells on endometrial CAFs. We demonstrated that CAF-mediated resistance to antitumor drugs occurs via direct and indirect contact with CAFs in HyCC. Here, we present the strength of our novel 2-cell HyCC model of patient-derived CAFs in solid tumors and provide a model to test the drug resistance tailored on a patient-to-patient basis.

Authors' Contribution

RS: The pathologist provided the evaluation of CAF based

on IHC staining. JCA: JCA performed the flow cytometry work. JCA supervised the ex vivo study logistics and helped in the EndNote library. XL: Research Assistant Lead standardized and performed tissue processing, ICC staining for CAF markers, H&E stains, and IHC. XL maintained the record of the histology work. AD: Research Associate obtained consent from patients and provided technical assistance in record keeping. AD helped in the preparation of figures, tables, and statistical correlations. KG: Provided insight into the overall logistical management of the ex vivo study and coordinated the clinical logistics of the study. LRE: The surgeon provided clinical insight into endometrial and ovarian tumors and corresponding blood samples. DS: The surgeon provided clinical insight into endometrial and ovarian tumors and corresponding blood samples. PD: Senior Scientist interrogated the genomic alteration of each tumor sample and matched the genomic alteration with the drug combination for the testing. PD helped in the analysis of data and writing the MS. ND: Senior Scientist conceptualized and supervised the study, wrote the MS, and analyzed the data.

Acknowledgments

We acknowledge Avera Cancer Institute for funding the entire study. We acknowledge every patient and their family for their participation in the ex vivo study at the Avera Cancer Institute.

Funding

The study was funded entirely by Avera Cancer Institute.

Institutional Review Board Statement

Anonymized tissue samples were collected at surgery from patients with endometrial cancers following their Informed (IRB approved: Protocol Number Study: 2017.053-100399_ExVivo001) consent.

Informed Consent Statement

Informed (IRB approved: Protocol Number Study: 2017.053-100399_ExVivo001) consents for receiving resected tissue were obtained from 72 enrolled patients with endometrial cancers.

Conflicts of Interest: None

Patent Status

The study presented in the MS is part of a patent application (United States Patent and Trademark Office; Application number 16/875,910).

References

- Brooks RA, Fleming G F, Lastra RR, et al. Current recommendations and recent progress in endometrial cancer. *CA Cancer J Clin* 69 (2019): 258-279.
- Connor E V, Rose P G. Management Strategies for Recurrent Endometrial Cancer. *Expert Rev Anticancer Ther* 18 (2018): 873-885.
- de Visser K E, Joyce J A. The evolving tumor microenvironment: From cancer initiation to metastatic outgrowth. *Cancer Cell* 41 (2023): 374-403.
- Chhabra Y, Weeraratna A T. Fibroblasts in cancer: Unity in heterogeneity. *Cell* 186 (2023): 1580-1609.
- Winterhoff B, Konecny G E. Targeting fibroblast growth factor pathways in endometrial cancer. *Curr Probl Cancer* 41 (2017): 37-47.
- Dzobo K, Dandara C. Broadening Drug Design and Targets to Tumor Microenvironment? Cancer-Associated Fibroblast Marker Expression in Cancers and Relevance for Survival Outcomes. *OMICS* 24 (2020): 340-351.
- Herrera M, Berral-Gonzalez A, Lopez-Cade I, et al. Cancer-associated fibroblast-derived gene signatures determine prognosis in colon cancer patients. *Mol Cancer* 20 (2021): 73.
- Sulaiman R, De P, Aske J C, et al. A CAF-Based Two-Cell Hybrid Co-Culture Model to Test Drug Resistance in Endometrial Cancers. *Biomedicines* 11 (2023): 11051326.
- Sulaiman R, De P, Aske J C, et al. Characterization and Clinical Relevance of Endometrial CAFs: Correlation between Post-Surgery Event and Resistance to Drugs. *Int J Mol Sci* 24 (2023): 24076449.
- Karpel H C, Slomovitz B, Coleman R L, et al. Treatment options for molecular subtypes of endometrial cancer in 2023. *Curr Opin Obstet Gynecol* 35 (2023): 270-278.
- Rubinstein M, Shen S, Monk B.J, et al. Looking beyond carboplatin and paclitaxel for the treatment of advanced/recurrent endometrial cancer. *Gynecol Oncol* 167 (2022): 540-546.
- Markman M, Fowler J. Activity of weekly paclitaxel in patients with advanced endometrial cancer previously treated with both a platinum agent and paclitaxel. *Gynecol Oncol* 92 (2004): 180-182.
- Kaznatcheev A, Peacock J, Basanta D, et al. Fibroblasts and alectinib switch the evolutionary games played by non-small cell lung cancer. *Nat Ecol Evol* 3 (2019): 450-456.
- Li C, Teixeira A F, Zhu H J, et al. Cancer associated-fibroblast-derived exosomes in cancer progression. *Mol Cancer* 20 (2021): 154.
- Richards K E, Zeleniak A E, Fishel M L, et al. Cancer-associated fibroblast exosomes regulate survival and proliferation of pancreatic cancer cells. *Oncogene* 36 (2017): 1770-1778.

16. Mao X, Xu J, Wang W, et al. Crosstalk between cancer-associated fibroblasts and immune cells in the tumor microenvironment: new findings and future perspectives. *Mol Cancer* 20 (2021): 131.
17. Chen Y, McAndrews K M, Kalluri R. Clinical and therapeutic relevance of cancer-associated fibroblasts. *Nat Rev Clin Oncol* 18 (2021): 792-804.
18. Orimo A, Gupta P B, Sgroi D C, et al. Stromal fibroblasts present in invasive human breast carcinomas promotes tumor growth and angiogenesis through elevated SDF-1/CXCL12 secretion. *Cell* 121 (2005): 335-348.
19. Xu Y, Li W, Lin S, et al. Fibroblast diversity and plasticity in the tumor microenvironment: roles in immunity and relevant therapies. *Cell Commun Signal* 21 (2023): 234.
20. Ravichandra A, Bhattacharjee S, Affo S. Cancer-associated fibroblasts in intrahepatic cholangiocarcinoma progression and therapeutic resistance. *Adv Cancer Res* 156 (2022): 201-226.